Fish and Shellfish Immunology 84 (2019) 756–767

Contents lists available at ScienceDirect

Fish and Shellfish Immunology

journal homepage: www.elsevier.com/locate/fsi

Full length article

Gold nanoparticles (AuNP) exert immunostimulatory and protective effects in shrimp (*Litopenaeus vannamei*) against *Vibrio parahaemolyticus*

M. Tello-Olea[a], S. Rosales-Mendoza[b], A.I. Campa-Córdova[a], G. Palestino[b], A. Luna-González[c], M. Reyes-Becerril[a], E. Velazquez[a], L. Hernandez-Adame[a,d], C. Angulo[a,*]

[a] *Immunology & Vaccinology Group, Centro de Investigaciones Biológicas del Noroeste, Instituto Politécnico Nacional 195, Playa Palo de Santa Rita Sur, La Paz, B.C.S, 23090, Mexico*

[b] *Sección de Biotecnología, Centro de Investigación en Ciencias de la Salud y Biomedicina, Universidad Autónoma de San Luis Potosí, Av. Dr. Manuel Nava 6, SLP, 78210, Mexico*

[c] *Centro Interdisciplinario de Investigación para el Desarrollo Integral Regional-Instituto Politécnico Nacional, Blvd. Juan de Dios Bátiz Paredes #250, Guasave, Sinaloa, Mexico*

[d] *CONACyT-Centro de Investigaciones Biológicas del Noroeste, Instituto Politécnico Nacional 195, Playa Palo de Santa Rita Sur, La Paz, B.C.S, 23090, Mexico*

ARTICLE INFO

Keywords:
Crustacean
Diseases
Metallic nanoparticles
Immunostimulants
Immune response
Acute hepatopancreatic necrosis disease
AHPND

ABSTRACT

Gold nanoparticles (AuNP) stimulate immune responses in mammals but they have not been tested in species of relevance in aquaculture. In this study the immunostimulant and protective potential of orally administered AuNP against *V. parahaemolyticus*, the causative agent of Acute Hepatopancreatic Necrosis Disease, was determined in shrimp. Synthetized AuNP (18.57 ± 4.37 nm) were moderately dispersed with a negative ζ potential of −10.3 ± 0.208 mV (pH = 7). AuNP were administered (single dose) at 0.2, 2, and 20 μg/g feed in shrimp. Hemolymph samples were withdrawn daily for 6 days. Hemolymph or hemocytes were used to determine total hemocyte counts, immune-related enzymatic activities, and expression of immune-relevant genes. Hepatopancreas was sampled for the analysis of AuNP biodistribution and histological examination. Survival was recorded daily. No mortality or toxicity signs in hepatopancreas were found. AuNP were detected in hepatopancreas. Early (24–48 h) immunostimulation was mainly related to immune gene up-regulation. Upon a challenge with *V. parahaemolyticus*, survival was higher (80%) and histopathological damages were lower in shrimp treated with the 2 μg/g dose when compared to the control. Therefore orally administered AuNP are proposed as immunostimulants that protect shrimp against *V. parahaemolyticus* infection.

1. Introduction

Shrimp (*Litopenaeus vannamei*) is one of the most cultivated species in aquaculture; activity in which pathogens cause high mortality and prominent economic losses. Thus new strategies to prevent or combat infectious diseases are required [1]. Recently *Vibrio parahaemolyticus* became one of the most relevant pathogens for the shrimp industry worldwide [2,3].

Several studies have reported a *V. parahaemolyticus* strain that acquired a plasmid (pVA1) coding for a binary toxin (PirAB-like toxin), which is similar to the PirAB toxin produced by *Photorhabdus luminescens* [4]. PirAB-like toxin-producing *V. parahaemolyticus* strains provoke the Acute Hepatopancreas Necrosis Disease (AHPND); characterized by severe atrophy of the hepatopancreas with massive detachment of epithelial cells, hemocyte infiltration, and necrosis [5]. Control of AHPND should be directed towards developing alternative strategies to antibiotics due to the risk of generating resistant strains and residues in food [6]. An attractive alternative is based on the use of immunostimulants, which enhance disease resistance by accelerating the recognition and elimination of pathogens by the immune system [7]. In shrimp, improved immunity has been demonstrated by the administration of immunostimulants such as β-glucans and lipopolysaccharides [7,8]. Cellular and humoral immune responses in shrimp mainly include the recruitment of hemocytes as well as increased phagocytic, phenol oxidase, and antioxidant enzymatic activities; among others [9,10].

Nanoparticles (NPs) (size up to 100 nm) have gained interest as antimicrobials, drug delivery vehicles, and immunostimulants [11,12]. Gold nanoparticles (AuNP) are one of the most stable and promising metal particles. The evidence suggests that the immune system cells

* Corresponding author.
E-mail address: eangulo@cibnor.mx (C. Angulo).

https://doi.org/10.1016/j.fsi.2018.10.056
Received 9 August 2018; Received in revised form 19 October 2018; Accepted 22 October 2018
Available online 24 October 2018

Table 1
Primers used in real time PCR.

Gen	Abbreviation	#Gen Bank	Forward (F)/Reverse (R) sequence
Toll like receptor	TLR3	JN180638.1	5′-GCTCGACATTTCAAATAACCG-3′ 5′-GA TTTGAGTTCGTTGTAGGAGAG-3′
Prophenoloxidase	ProPO	AY723296	5′-ACTGGCACTGGCACCTGA -3′ 5′-TTTGGCAGCGTGTTGTCC-3′
Ribosomal protein	RFLP7	AFU93449.1	5′-GCACTGTTTTGGTTCCTG-3′ 5′-TGATGGTCTTCAGGTTGG-3′

interact with metal nanoparticles through Toll-like receptors (TLRs) in both vertebrates and invertebrates [13–15]. In addition, the effect of naked AuNP on cell proliferation, cytotoxicity, and immune response has been investigated. In human peripheral blood mononuclear cells, the administration of AuNP activates immune-related genes [16]. *In vitro* studies using mouse cells revealed that naked AuNP induced proliferation of keratinocytes, activation of phagocytes, expression of pro-inflammatory cytokines, and maturation of neutrophils [17,18]. Moreover, the oral administration of AuNP in mouse increases cell proliferation and secretion of pro-inflammatory cytokines [19,20]. Regarding shrimp, only silver nanoparticles have been studied. Shrimp fed with silver nanoparticles (AgNP) showed increased total hemocytes count, expression of immune-related genes, and resistance to a *V. parahaemolyticus* challenge [21]. Therefore this study was focused on determining in shrimp the effect of the oral administration of naked gold nanoparticles (AuNP) on the immune response and protection against *V. parahaemolyticus* experimental infection.

2. Materials and methods

2.1. Synthesis and characterization of gold nanoparticles

Chloroauric acid ($HAuC_{l4}$; 99.9%), sodium citrate, and ultra-purified Milli-Q® water were used to prepare AuNP. The synthesis was carried out using the Turkevich method that produces high quality AuNP [22]. AuNP were analyzed by spectroscopy using a UV-Vis spectrophotometer (Cary 60, Agilent Technologies®, Silicon Valley, CA). The optical spectra were obtained by using a standard halogen lamp (Thorlabs 150 W) in a 5 mm quartz cuvette. The size and shape were studied by Transmission Electron Microscopy (TEM) using a JEOL® jem-1230 microscope (USA), equipped with an Energy-dispersive X-ray (EDS) accessory for an elemental analysis of the sample. The stability and zeta potential of AuNP were analyzed by Dynamic Light Scattering (DLS) using a Nano S90 ZetaSizer (Malvern Aimil Instruments Pvt Ltd, Malvern, UK) equipment at the following concentrations: 0.2, 2, and 20 μg of AuNP per mL of Milli-Q® water.

2.2. Vibrio parahaemolyticus strain

The *V. parahaemolyticus* strain IPNGS16 used in this study was isolated from shrimp with typical signs of AHPND during an outbreak in shrimp farms in Sinaloa, Mexico López-León et al. (2016) [23]. *V. parahaemolyticus* was cultured in TSB BD BIOXON® (New Jersey, USA) medium with 2.5% NaCl. To confirm the bacterial species, a sample was seeded by cross-striking in CHROMagar®, as well as in TCBS agar specific for *Vibrio*, and cultured at 35 °C for 18 h. Additionally, Gram staining was performed to confirm bacterial cell morphology. To corroborate the presence of the Pir-AB toxin gene in the bacterial strain, genomic DNA was extracted using the FAST DNA® Spin Kit and a nested PCR was performed [24].

For the bacterial challenge, *V. parahaemolyticus* was cultured in TSB with 2.5% NaCl at 30 °C for 18 h and centrifuged at 3779 × *g* for 20 min. The cell biomass was resuspended in saline water (2.5% NaCl) and the optical density at 595 nm was adjusted to 1.0, which corresponds to 1.65×10^7 CFU/mL.

2.3. Animals and experimental AuNP supplemental diets

Shrimps with 7.05 ± 0.5 g of body weight were used. Animals were kept in 60 L tanks containing 40 L of seawater under de following conditions: salinity of 37 ± 1% units of salinity (ups), 25 ± 1 °C (30 ± 1 °C for the bacterial challenge test), dissolved oxygen (OD) > 6 mg/L, and 40% replacement of water every 48 h. Commercial feed Camaronina Purina® (Minnesota, USA) was used and animals were fed with 3% of the total shrimp weight twice a day during the acclimation and experimental periods. CIBNOR Bioethical Committee approved the experiments performed in this study.

The AuNP doses used were established based on previous *in vivo* studies in which no cytotoxic effects were found. AuNP concentrations were established using a 9.96 mM AuNP suspension, which was diluted in sterile Milli-Q® water and applied to the feed by aspersion as previously described [25]. Feed was subsequently dried at room temperature and stored at 4 °C until further use.

2.4. Experimental immunological bioassay

Four shrimp groups were established (45 per group, n = 15 shrimp by replicate). Treatments comprised three concentrations of AuNP (0.2, 2, and 20 μg/g of diet) and a control condition (diet without AuNP). A single dose (3% total shrimp weight) containing 0–20 μg of AuNP was administered to shrimp by feeding. Feed residues and feces were eliminated 48 h post-administration. Three shrimp per tank were sampled at 0, 24, 48, 72, 96, and 120 h post-administration. Hemolymph samples were withdrawn to determine total hemocyte counts, immune-related enzymatic activities, and expression of immune-relevant genes. Hepatopancreas was sampled for the analysis of AuNP biodistribution and histological examination. Mortality was daily recorded throughout the experiments.

2.5. Immunological analysis

2.5.1. Total hemocyte count (THC)

A known quantity of hemolymph with anticoagulant was taken and fixed with 4% formaldehyde. THC was performed in a Petroff Hausser Scientific® counting chamber under a Light microscope Olympus (Tokyo, Japan). Dilution factor calculations were performed on each sample to determine the number of cells per milliliter.

2.5.2. Superoxide dismutase (SOD) activity

Hemolymph samples were centrifuged at 800 × *g*. Phosphate buffer (500 mM, pH 7.8) was added to the pellet and homogenized with a Polytron® (Montreal, Canada). Samples were then centrifuged at 5800 × *g* for 5 min and supernatants collected; these were analyzed using the SOD kit (Sigma-Aldrich®) according to the instructions from the manufacturer using 96-well microplates. SOD activity was expressed as units of inhibition percentage where one unit of SOD/mL reduces the rate of WST-1 formazan formation by 50%.

2.5.3. Peroxidase activity

Peroxidase activity was measured in hemolymph supernatants by microplate colorimetric method [26]. Briefly, 20 μL of supernatant were

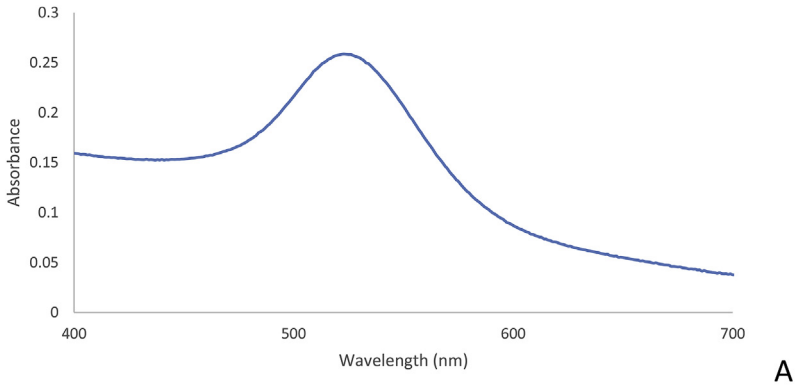

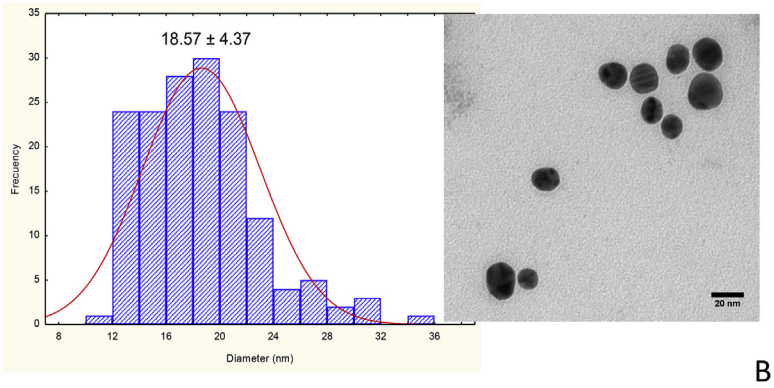

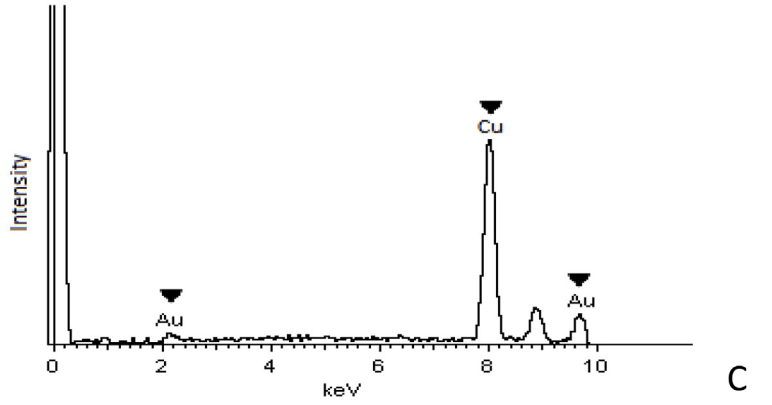

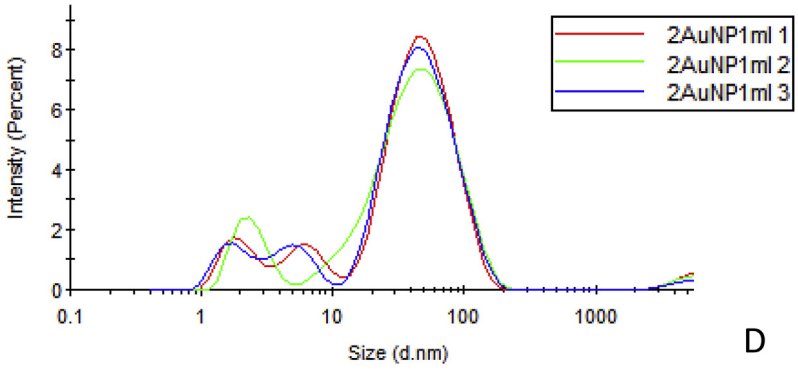

Fig. 1. Characterization of gold nanoparticles. (A) UV-Visible spectrum of AuNP. (B) Morphological analysis of AuNP; Right: TEM image of gold nanoparticles synthetized by the Turkevich method, showing an ovoid shape. Left: Size distribution histogram shows an average particle size of 18.57 ± 4.37 nm. The Image J software was used to analyze TEM images. (C) EDS spectrum of gold nanoparticles. The peak positions of elemental Au are indicated by ▼ marks. (D) DLS of AuNP showing the hydrodynamic diameter of AuNP. (For interpretation of the references to color in this figure legend, the reader is referred to the Web version of this article.)

Table 2
ζ potential data of gold nanoparticles as function of pH.

pH	mV	S.D.
1	3.58	1.7
3	−4.32	0.118
5	−14.7	0.954
7	−10.3	0.208
9	−7.07	0.408

mixed with the peroxidase substrate (80 μM 3.3′,5,5′-tetramethylbenzidine hydrochloride, TMB, Sigma®, containing 2.5 mM H_2O_2). The reaction was stopped after 5 min by adding 50 μL of 2 M H_2SO_4. The optical density was measured at 450 nm. The activity unit was defined as a change in one unit of optical density values.

2.5.4. Catalase activity

Catalase activity was measured as previously described [27]. Briefly, each sample was mixed with assay phosphate buffer and methanol. Then, H_2O_2 (Applichem) was added and incubated at room temperature for 20 min under continuous stirring. Afterwards, potassium hydroxide and Purpald solution (Sigma-Aldrich®, St. Louis, MO, USA) was added to develop the reaction at room temperature for 35 min with continuous stirring. A solution of potassium periodate (Sigma-Aldrich®) diluted in KOH was subsequently added to oxidize the formaldehyde-purpald complex and absorbance at 595 nm was measured after 5 min of incubation.

2.6. Immune-related gene expression analysis

2.6.1. RNA extraction and cDNA synthesis

RNA extraction from hemocytes was performed according to the Trizol Reagent protocol (Sigma-Aldrich®) with some modifications. Hemocytes were lysed and centrifuged at 12000 × *g* for 10 min. Afterwards, chloroform was added and centrifuged at 12,000 × *g* for 15 min to separate the aqueous phase; which was subsequently precipitated overnight with one volume of 2-propanol. The pellet was resuspended in sterile Milli-Q® water and RNA was quantified at 260 nm in a Nano Drop (NanoDrop Technologies, Wilmington, DE). RNA samples were treated with DNAse I (Sigma-Aldrich, St Louis Missouri, USA) to remove residual genomic DNA. cDNA synthesis was performed according to the Improm II Promega® protocol (Wisconsin, USA) using 1 μg of total RNA. The cDNA obtained was stored at −20 °C until further use.

2.6.2. Real-time PCR (qPCR)

cDNA was used to quantify the expression of Toll-like receptor 3 (TLR3) and prophenoloxidase genes by qPCR. Ribosomal protein L7 (RPL7) gene was used as endogenous control. Table 1 shows the primers designed for this study. The qPCR was carried out in a Real Time PCR System Rotor gene 6000 (Qiagen, Netherlands, Germany) using SSOfast Eva Green Bio-Rad®. Amplifications were carried out in a reaction volume of 15 μL containing 7.5 μL of master PCR mixture, 10 μM of each specific primer (Forward/Reverse), and 5 μL of cDNA dilution. The amplification program comprised the following steps: 95 °C for 5 min followed by 40 cycles of 95 °C for 15 s, 60 °C for 20 s, and 72 °C for 25 s. Each sample was run in triplicate for each gene. Reactions without cDNA were included as negative controls for each set of primers.

The relative amounts of all target transcripts were calculated according to the 2ΔΔCT method [28]. mRNA levels were normalized to the levels of the RFLP7 gene and expressed as relative level: (Target mRNA expression)/(control mRNA expression). The results are presented as the mean ± standard error (S.E.).

2.7. Toxicity analysis of AuNP in shrimp by histopathology

Whole organisms were fixed in reactive Davidson solution [29]. Three organisms per group were taken before (0 h) and after (120 h, end of the experiment) AuNP oral administration. Afterwards, each organism was dissected and the hepatopancreas recovered. Samples were dehydrated, embedded in paraffin, and cut in 4-μm thick sections. Hematoxylin and eosin staining was performed on each sample and observed with an Olympus BX41 optical microscope® (Tokyo, Japan) integrated with a NIKON® camera. Images were taken at 20× and 40× objectives for histological examinations.

2.8. AuNP detection in shrimp by confocal laser scanning microscopy

Visualization of AuNP in hepatopancreas was carried out as previously described [30]. Histological tissue samples were processed as described above but omitting the staining step. 4 μm histological slide samples were analyzed in an inverted confocal laser scanning microscope Leica TCS SP8 (40x, Leica, Wetzlar, Germany) under reflection mode using the 10× objective. Laser wavelength within the spectrum of visible light (Argon 514 nm, 20% power) was used to excite AuNP in the tissue. Light scattering was recorded in the channel with a filter of long pass, 505 nm emission. Images were taken at five different spots of the histological slide samples. Histological slides without AuNP were used as control to adjust the detector gain and establish the baseline.

2.9. Challenge with V. parahaemolyticus

Bacterial challenge was conducted as previously described [31]. Five experimental groups (n = 10 shrimp by replicate) were organized as follows: (1) Negative control group (saline solution), (2) Positive control group (*V. parahaemolyticus* challenge only), (3) group receiving 0.2 μg/g AuNP and challenged with *V. parahaemolyticus*, (4) group receiving 2 μg/g AuNP and challenged with *V. parahaemolyticus*, and (5) group receiving 20 μg/g AuNP and challenged with *V. parahaemolyticus*. Shrimps were fed once with diet supplemented with AuNP. After 24 h, shrimp were challenged with a *V. parahaemolyticus* LD_{50} dose ($LD_{50} = 9 \times 10^5$ UFC/mL). At the end of the experiment (36 h), samples from shrimp survivors were taken for histopathological analysis as described below. The mortality was recorded every 3 h over a 36 h period and the survival rate was calculated by the following formula:

Survival percentage (%) = 100 - [(Number of death shrimp after challenge/Number of shrimp) × 100].

2.10. Histopathological analysis after bacterial challenge

Quantitative analysis was performed to evaluate the differences on

Table 3
Morphometric parameters applied in the quantitative analysis of histological hepatopancreas images in shrimp (L. vannamei).

Morphometric parameter	Description
Tubular diameter (TD)	Total area covered by epithelium that include B, F and R cells.
Number of infiltrated hemocytes (NIH)	Quantity of hemocytes present on analyzed images.
Number of septic nodules (NSN)	Number of hemocyte clusters on analyzed images.
Height of tubular epithelium	Distance comprising tubular epithelium towards basal area of the lumen.

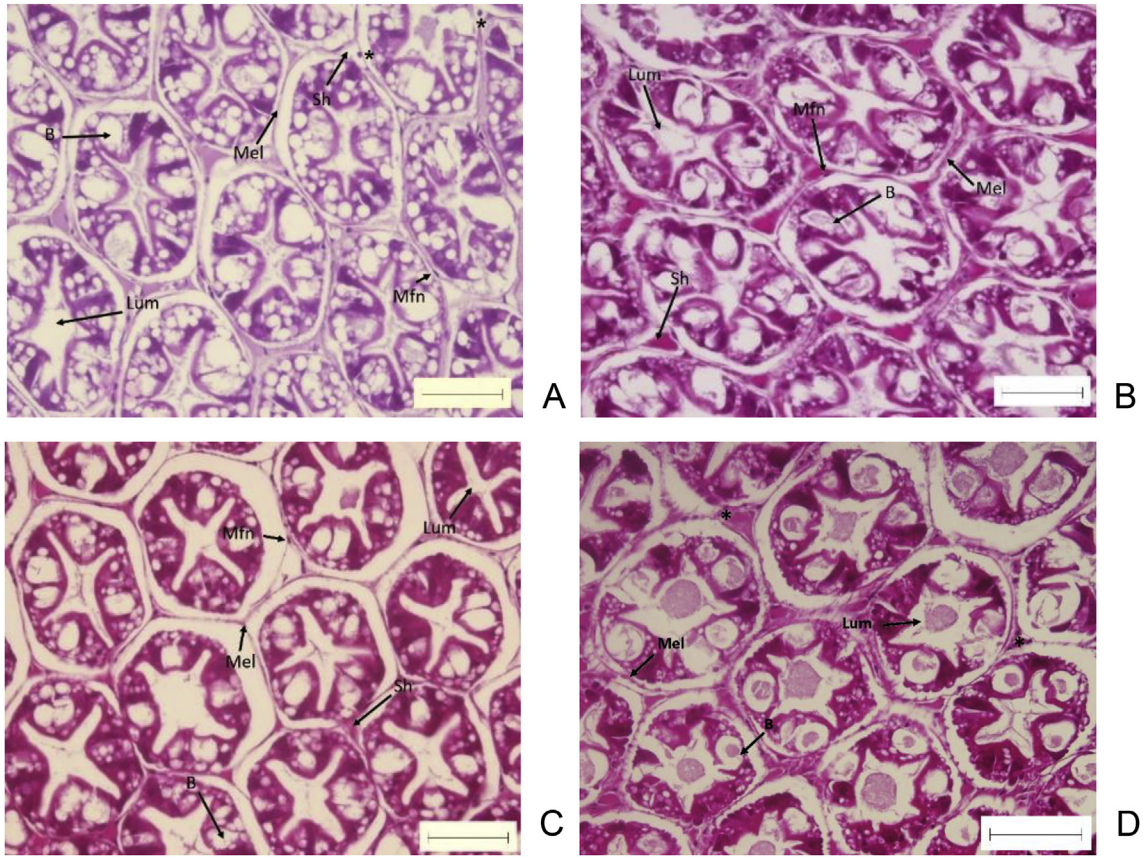

Fig. 2. Cross-sectional micrograph of hepatopancreas from shrimp fed control diet (without AuNP) or AuNP-supplemented diet at different concentration at 120 h. A) Control; B) 0,2 μg/g; C) 2 μg/g and D) 20 μg/g. Tubule (T); Myoepithelial layer (Mel); Lumen (Lum); B cells (B); Myoepithelial cells (Mfn); Sinus hemal (Sh); Hemocytes (*). H & E staining. Bar length = 200 μm.

damage level among experimental groups. Five images (40× objective) for each organism were observed in the experimental groups. The analyzed images were randomly selected to avoid biases in the analyses. The morphometric parameters found in the analyzed images of the positive controls were selected for the quantification of the main morphological changes observed in the hepatopancreas during infection with *V. parahaemolyticus* (Table 3). Image ProPlus V.6.0 software was used to analyze images.

2.11. Statistical analysis

Data were statistically analyzed in the R program, RStudio® platform, to determine significant differences among different treatments. Homogenicity (Shapiro) and homocedasticity (Fligner) tests were performed. Kruskal Wallis or 1-way ANOVA tests were performed for enzymatic, gene expression, and quantitative histopathology analyses. Post-hoc tests (Tuckey and Dunn test) were performed to assess significant differences among treatments. Differences were considered significant when $p < 0.05$. Results were expressed as mean ± standard error.

3. Results

3.1. 18-nm AuNP were successfully synthetized

The synthetized AuNP were subjected to a characterization by several techniques. First the UV-Vis spectrum shown in Fig. 1A depicts an optical absorption band centralized at 526 nm. The shape and size of the AuNP were analyzed by the TEM images shown in Fig. 1B (I). The micrographs confirmed spherical AuNP with a 10–32 nm size range. The average size was 18.57 ± 4.37 nm (Fig. 1B). EDS spectrum confirmed the presence of the two representative peaks of Au (2.2 and 9.7 KeV, see Fig. 1C), which confirms AuNP free of impurities. The peak observed at 8 KeV represents the spectrum of Cu that corresponds to the grid used for the measurements. In Fig. 1D the hydrodynamic diameter of the AuNP can be observed. There is a 3 sizes dispersion, whose highest intensity is at a diameter of 54.82 nm (Pdi = 0.617). The ζ potential was determined at different pH values; the nanoparticles are highly stable and have a negative surface charge in almost the entire pH range as shown in Table 2.

3.2. AuNP are not inherently toxic for shrimp (L. vanammei)

During the course of the bioassay, no mortality was observed in any of the experimental AuNP doses and control groups. In addition, histological examinations of hepatopancreas samples showed no signs of damage or toxicity. In this study, normal tubules (T) delimited by the myoepithelial layer (Mel) and a star-shaped lumen (Lum) were observed upon oral administration of AuNP, as well as a large number of B cells (B) and some myoepithelial cells (Mfn). The presence of some hemocytes (asterisks) in the tissue was detected 120 h post-treatment (Fig. 2).

3.3. AuNP localize in hepatopancreas cells of shrimp treated with the highest test dose

In the confocal microscopy analysis, AuNP were not detected in the hepatopancreas from control shrimp (Fig. 3). In contrast, scattering signals were observed in hepatopancreas of shrimp fed with AuNP using the highest test dose (20 μg/g feed) at 120 h post-AuNP administration

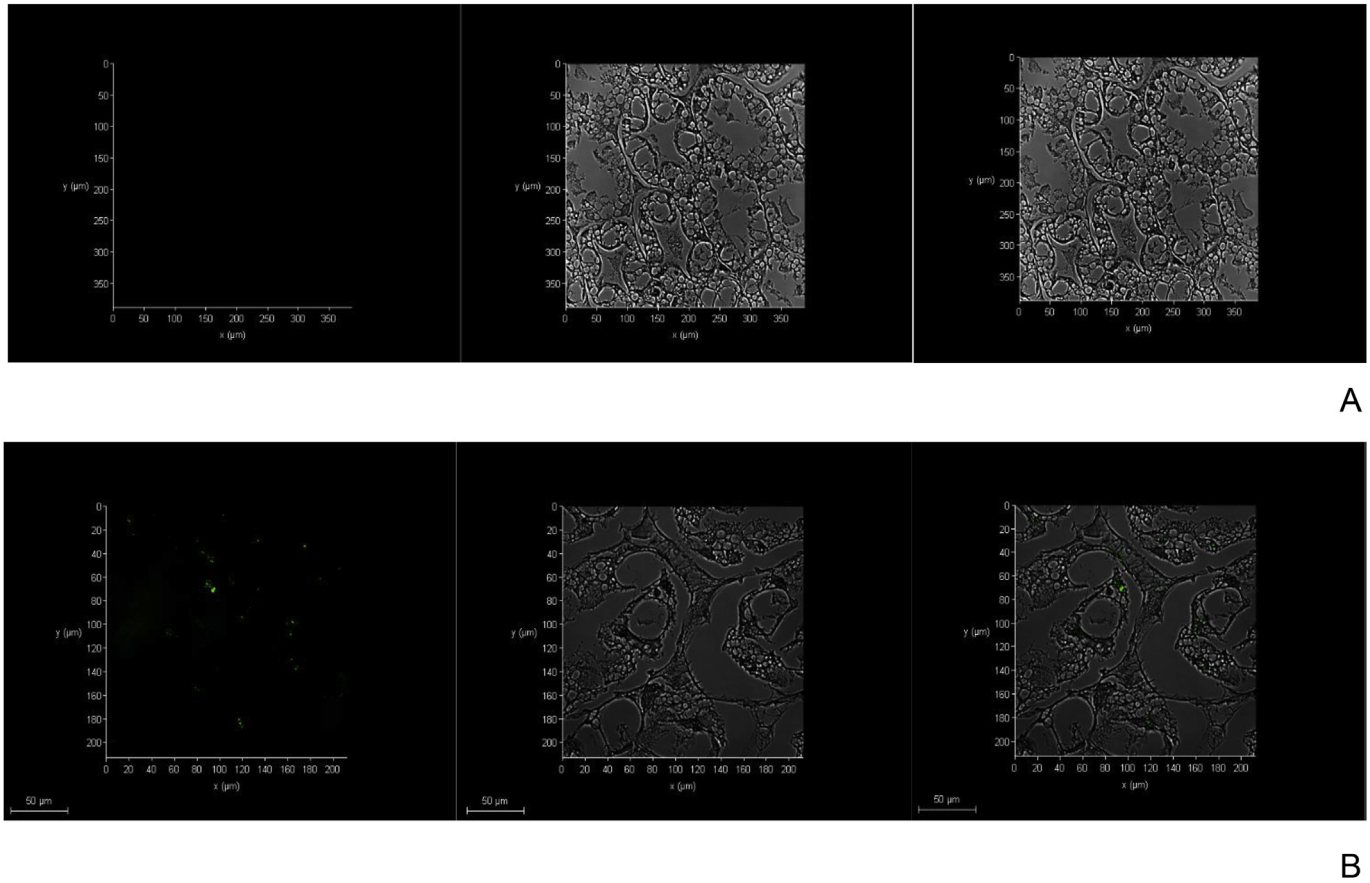

Fig. 3. CLSM images of AuNP in hepatopancreas of shrimp at 120 h post-feeding. A) control treatment (food without AuNP) and B) AuNP 18 nm at 20 µg/g. Scale bar length is 50 µm. Left: fluorescence image; Middle: optical image; Right: merged images.

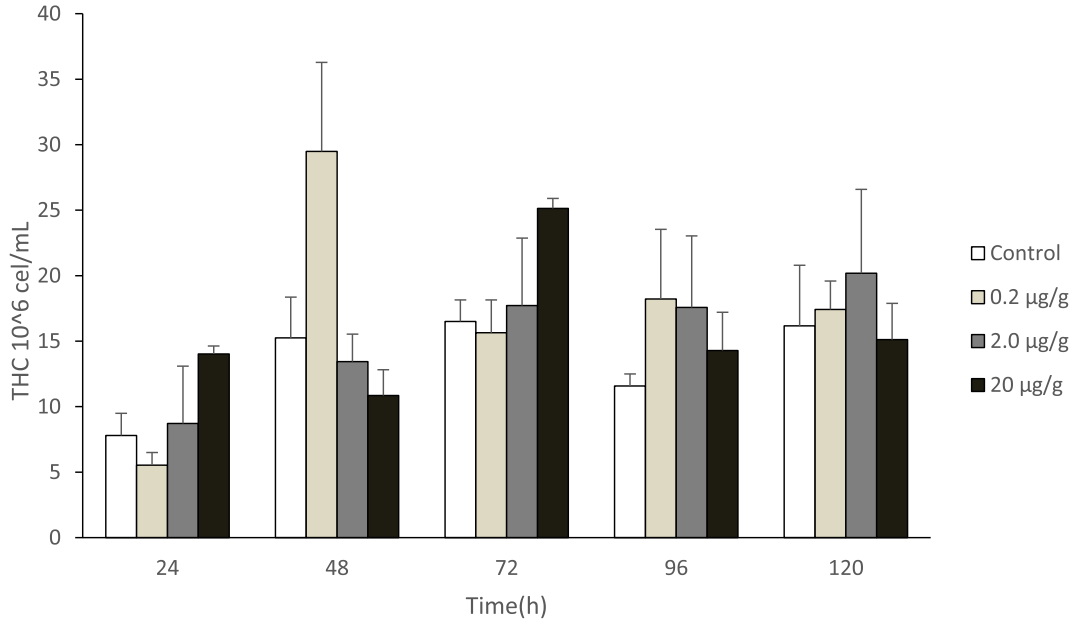

Fig. 4. Total hemocyte counts of shrimp orally treated with AuNP. Shrimp were fed once with standard feed or feed supplemented with AuNP at 0.2, 2.0, and 20 µg/g feed. Ctrl = Group control without nanoparticles; Each bar represents the mean value from eight shrimp. Data are presented as the mean ± S.E.

(Fig. 3 B).

3.4. AuNP modulate cellular and humoral immune parameters

An increase in the total hemocyte count (THC) was observed upon treatment with AuNP with respect to the control treatment. However, no statistically significant differences were found among treatments (Fig. 4). The activity of SOD, CAT, and myeloperoxidase in plasma of shrimp treated with AuNP was variable among treatments when compared to the control group throughout the study (Supplementary Tables

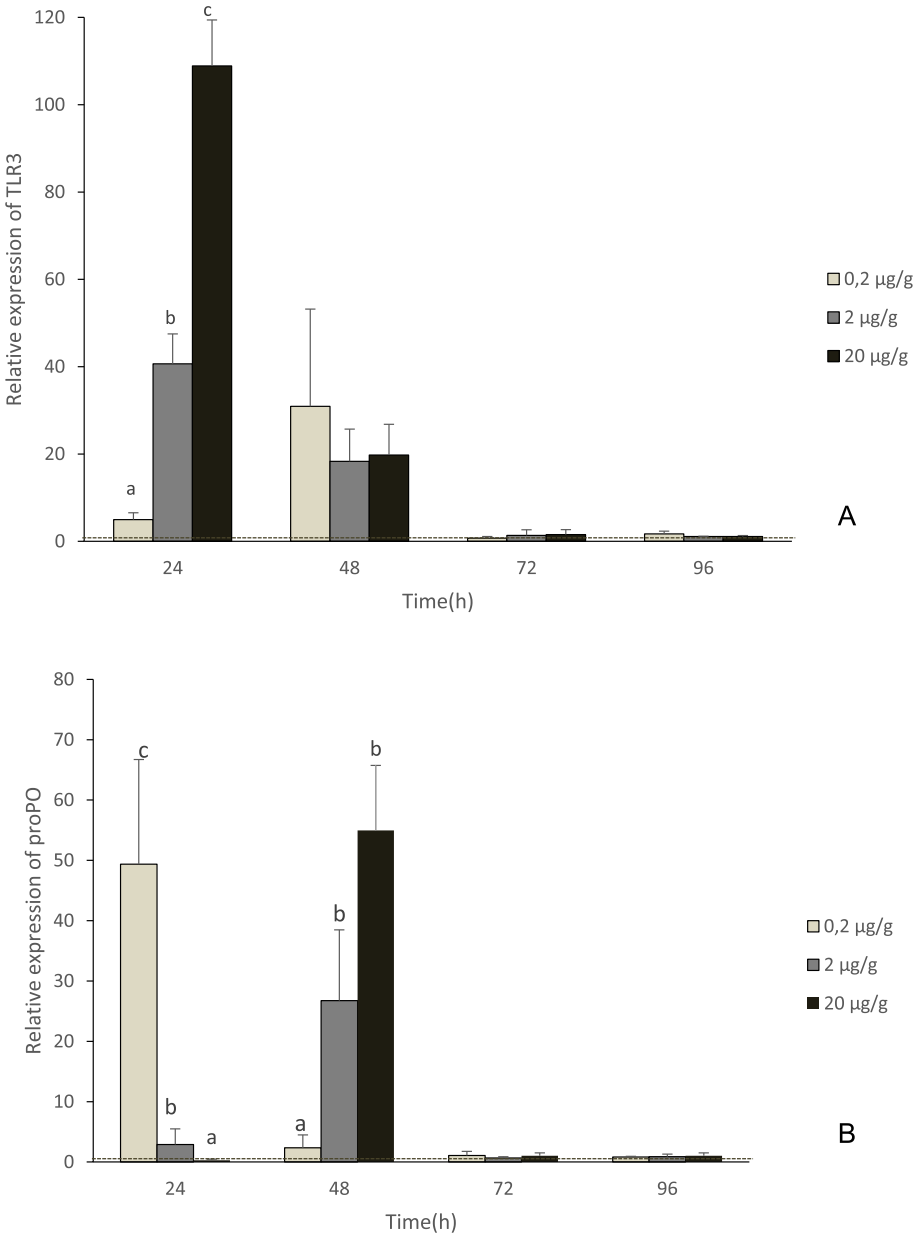

Fig. 5. Relative mRNA expression of (A) TLR3 and (B) proPO in white shrimp hemocytes in response to administration of AuNP on diet at concentrations of 0.2, 2, and 20 µg/g. Statistical differences are denoted by different letters ($p < 0.05$). Data are presented as the mean ± S.E. The mRNA levels were normalized to the levels of RPL7 gene and expressed as relative level: (Target mRNA expression)/(control mRNA expression).

S1–3).

3.5. The expression of TLR3 and ProPO genes is modulated in hemocytes

TLR3 gene expression in hemocytes from shrimp fed with AuNP showed a dose-dependent up-regulation ($p < 0.05$) at 24 h. Test shrimp subjected to the 20 µg/g dose presented the highest value with a 100-fold expression increase with respect to the control. TLR3 transcript levels in hemocytes at 48 h were similar among the AuNP treatments and then sharped to the levels reached by the control group at 72–96 h post-treatment (Fig. 5A). The expression of the proPO gene in hemocytes from shrimp fed with AuNP showed inverse dose-dependent effects at 24 and 48 h ($p < 0.05$). At 24 h, the highest proPO gene expression levels were observed in hemocytes from shrimp fed with the lowest AuNP dose, followed by the higher doses. In contrast, at 48 h, the highest mRNA transcription of proPO gene was found at the highest AuNP dose, followed by the lower doses. Thereafter (72 and 96 h), the proPO gene expression levels were similar among AuNP and control groups (Fig. 5B).

3.6. AuNP increased survival and decreased hepatopancreas damage of shrimp challenged with Vibrio parahaemolyticus

The *V. parahaemolyticus* IPNGEV16 strain was confirmed by TSBS and chromo agar, Gram stain, and the presence of genes coding for toxins PirA and PirB by PCR. In the challenge bioassay, survival was significantly ($p < 0.05$) higher (80%) in shrimp fed with AuNP at a 2 µg/g dose after infection with *V. parahaemolyticus* when compared to the positive control (10%, *V. parahaemolyticus* only) at 36 h. The uninfected control group showed 100% survival rate (Fig. 6). Shrimp fed with AuNP and challenged with *V. parahaemolyticus* showed less histopathological damage and hemocytic infiltration when compared to the positive control, especially in the group treated with the 2 µg/g dose (Fig. 7A–J). Interestingly this effect was not significant in the groups

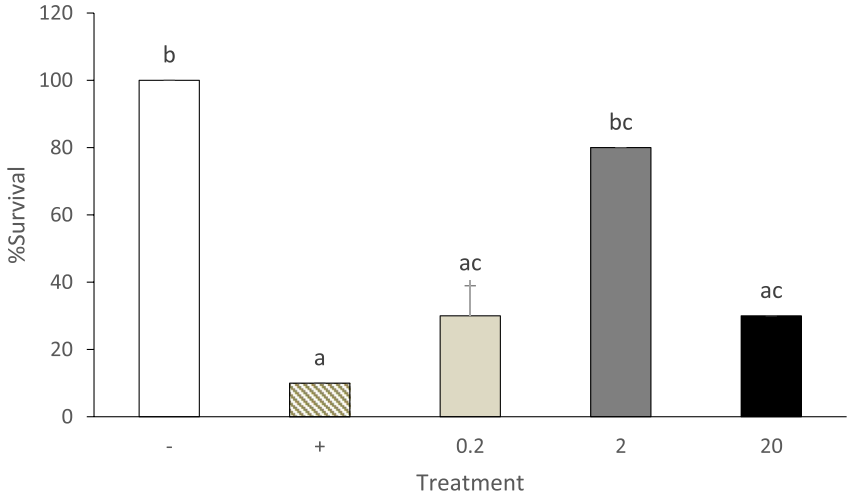

Fig. 6. Percentage survival of shrimp infected with *V. parahaemolyticus* strain (Time 36 h, LD50 dose = 9 × 10^5 CFU/mL). (−) Negative control, without bacteria + commercial feed; (+) positive control, bacteria + commercial feed; 0.2, 2, 20 μg/g AuNP used for the bioassay-challenge + infection with bacteria. Statistical differences are represent by different letters ($p < 0.05$). The results are presented as the mean ± S.E.

treated with 0.2 and 20 μg/g doses, which is in agreement with shrimp survival results. Quantitatively, the height of tubular epithelium and tubular diameter increased; while the number of infiltrated hemocytes and number of septic nodules decreased in the groups treated with 0.2 and 2 μg/g AuNP doses with respect to the infected control (Fig. 8).

4. Discussion

The size and shape of the AuNP are key parameters that influence their interaction and effects in biological systems [15,17]. In this study, the peak observed in the UV-Vis spectrum corresponds to the localized surface plasmon resonance (LSPR) of AuNP with a size of ~15 nm. This peak also shows a slight widening that indicates an increase in the size distribution due to a change in the particle shape [32,33]. The negative ζ potential of the synthesized AuNP can be ascribed to the adsorbed citrate anions on the AuNP surface, which facilitates the biological interaction with positively charged tissues [34].

Once synthetized and characterized, AuNP were orally administered to shrimp observing no mortality or signs of toxicity. On this regard, toxicity was assessed by histological analysis of hepatopancreas; which is a crucial organ in penaeid shrimp since it fulfills the functions of liver, pancreas, intestine, and other organs of vertebrates [35]. Hepatopancreas function involves the absorption and storage of nutrients, synthesis of digestive enzymes, and detoxification of xenobiotics [36]. Remarkably, AuNP interactions with cells and molecules are dynamic, which also mediate their accumulation and toxicity in mammals [37,38]. Despite that there are no reports regarding histological damages associated to AuNP or metal nanoparticles in shrimp, other toxicity studies are useful to interpret the absence or presence of toxicity signs. Recently, exposition of crustaceans *Artemia nauplii* and *A. salina* to AuNP (10–130 nm) for 48 h showed neither mortality nor toxicity signs [39,40]. Similar results were observed in fish fed with AuNP [41]. On the other hand, it has been reported that exposure to heavy metals, such as copper, induces histological changes in the hepatopancreas of *L. vannamei* [42–44]. In such reports, signs of damage comprised the reduction of R and B cells, epithelial cell shedding, and strong infiltration of hemocytes. Interestingly, in mouse low concentrations (137.5–2200 μg/kg body weight) of 13.5-nm AuNP (administered by different routes) did not cause toxicity even after prolonged periods [45]. Therefore, based on the results of the present study, it can be established that the oral administration of AuNP (18.57 nm in size) with doses in the 0.2–20 μg/g range has no toxic effects in shrimp.

To generate insights on the biodistribution of AuNP upon oral administration in shrimp, confocal microscopy was conducted in histological preparations of the hepatopancreas taking advantage of the AuNP optical properties due to the plasmon resonance. AuNP were detected in hepatopancreas from shrimp fed with the highest AuNP dose [30,46]. Morphology, particle size, and charge surface are crucial factors for biodistribution among the organs [47]. On this regard, AuNP were detected in the intestine of the crustacean *A. nauplii* 48 h after aqueous exposition and in the gastrointestinal tract of fish fed with AuNP [40,41]. Recently, Wade et al. demonstrated that AuNP were retained in the hepatopancreas up to 18 h following a single oral dose in *Penaeus monodon*; a phenomenon that largely depended on the nanoparticle size [48]. In rats, a single oral administration of 18-nm AuNP led to a 70% rate of NP excretion in feces at 24 h; in addition, the remaining AuNP were translocated into the circulatory system and mainly accumulated in heart and brain tissues; an effect related to the nanoparticle size [49]. Furthermore, studies in mice demonstrated that AuNP (13 nm in size) mainly localized in spleen and liver (hepatopancreas in shrimp being an analog organ that fulfills both functions) [35,47]. Although determining AuNP biodistribution and fate is a pending objective in shrimp (*L. vanammei*), efforts have been done in this direction using artemia models [39,40]. Thus, future experiments in shrimp will be performed to determine whether AuNP can be detected in other organs and tissues in short- and long-term studies; including hemocytes to elucidate their direct relationship with immune function. Remarkably, some immunostimulants are aggressive (toxic) to the host and may induce suppression of the immune response when used at high concentrations and daily exposure during long periods of time [50,51]. Thus, short-term trials are useful to select immunostimulants and doses, and thereafter frequency and periods of administration can be evaluated [52,53]. Overall, a better understanding of AuNP biodistribution and immunological-mediated mechanisms are needed for aquaculture and human health applications.

The invertebrate (innate) immune system comprises molecular and cellular (hemocyte) components. Circulating hemocytes in crustaceans play an important role in immunity; performing functions of phagocytosis, encapsulation, and lysis of foreign particles and cells [10]. Hemocytes are produced continuously in hematopoietic tissues and their levels vary dramatically during immunostimulation or infection [1,54]. In this study, the THC showed variations among the sampling times. On this regard, an increase in the THC in *L. vannamei* orally treated with silver nanoparticles (AgNPs) (0.1 mg per 10 mg food) has been observed when compared to the control group [21]. Clearly, oral treatment with metallic NP affects THC in shrimp and merits deeper investigation.

In addition, when a foreign particle is phagocytized by hemocytes the mechanism of respiratory burst can be activated; leading to the production of reactive oxygen species (ROS: O_2^-, H_2O_2, OH−) that mediate elimination of pathogens or foreign particles. However, the excess of ROS can also damage host cells [55]. The defense against ROS

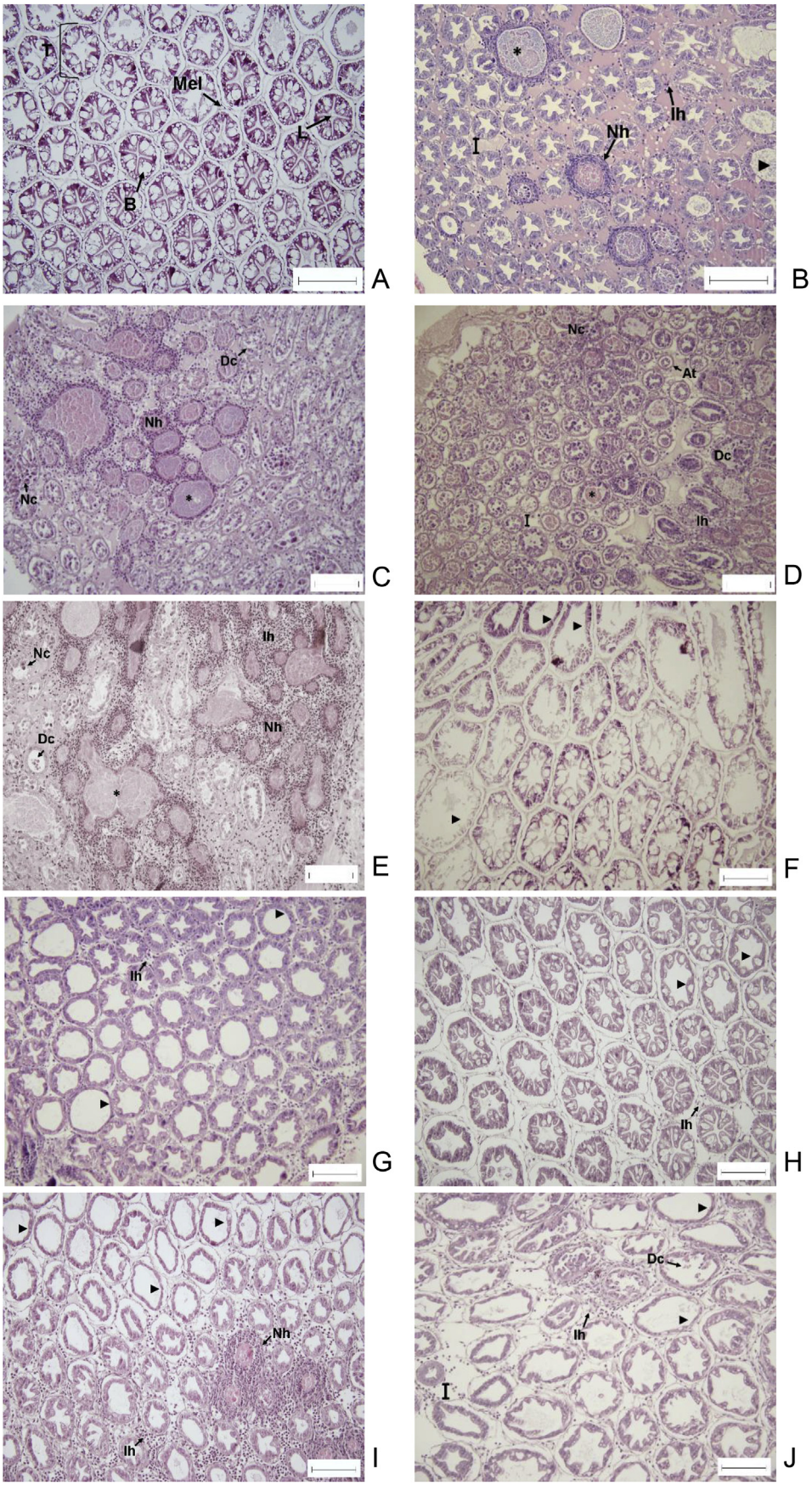

Fig. 7. Histopathological analysis of the hepatopancreas from shrimp infected by immersion with *V. parahaemolyticus* strain (Time 36 h, dose = 9 × 10 ˆ 5 CFU/mL). Hemocytic infiltration (ih), hemocytic nodules (nh), bacteria (*), epithelial cell detachment (Dc), lumen hypertrophy (▼), tubular atrophy (At), loss of tubular structure (I). A, control group: commercial feed without bacterial suspension; B—C-D, Positive control: commercial feed + bacterial suspension; E-F, G-H, I-J, Groups fed with AuNP (0.2, 2 and 20 μg/g) + bacterial suspension. Paraffin section of 4 μm, H & E staining. Bar length = 100 μM.

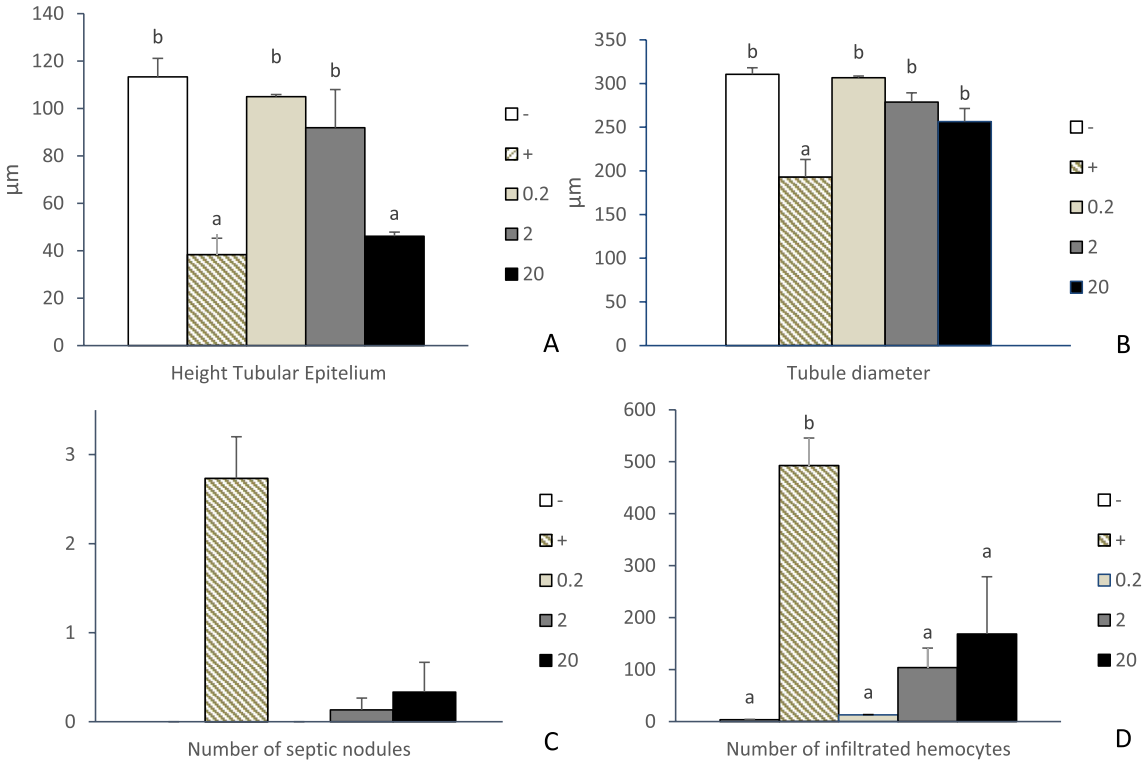

Fig. 8. Quantitative histological values of hepatopancreas from shrimp fed with AuNP (0.2, 2, and 20 µg/g) and experimentally infected with *V. parahaemolyticus*. (A) Height tubular epitelium; (B) Tubule diameter; (C) Number of septic nodules; and (D) Number of infiltrated hemocytes. Different letters indicate significant differences ($P < 0.05$). Data are presented as mean ± SE. *In (C), ANOVA data analysis could not be performed due to values of 0 found in control and 0.2 group.

comprises the activities of superoxide dismutase (SOD), catalase (CAT), and myeloperoxidase; among others [56]. SOD dismutates O_2^- in H_2O_2 and subsequently H_2O_2 is converted into oxygen and H_2O by catalase. Additionally, H_2O_2 is also processed by myeloperoxidase to generate hypochlorous acid; a highly toxic compound for phagocytosed pathogens. Therefore, an increase in the activity of these enzymes is associated with the stimulation of the immune system in shrimp. In this study SOD, CAT, and myeloperoxidase activities in plasma were highly variable among treatments, suggesting that the activity of these immune-related enzymes should be measured in other tissues to determine the global effect of orally administered AuNP on these relevant enzymatic activities. For example, previous studies found an increase in catalase activity in tissues (muscle and hepatopancreas) of the giant shrimp *Macrobrachium rosenbergii* supplemented with copper nanoparticles in the feed [57]. Similarly, increases in the respiratory burst activity of granulocytes and monocytes have been reported in mice fed with a colloidal suspension of AuNP at a 0.25 µg/g dose when compared to the control group [20].

On the other hand, the innate immune system triggers responses through signaling pathways that involve the interaction of receptors from the host and foreign molecules and culminates with an effector response [58]. For example, Toll-like receptors (TLRs) recognize different types of molecules or particles in both vertebrates and invertebrates [13,14]. In shrimp (*L. vannamei*), 3 Toll-like receptors (LvToll1, LvToll2 and LvToll-3) have been reported [59]. On the other hand, melanization is an effector immune response by the ProPO system, which starts by the recognition of foreign molecules by receptors in the host that culminate with the formation of melanin and the production of ROS to kill pathogens [9,60,61]. Moreover TLR and proPO genes are key biomarkers of innate immunity involved in protection of shrimp (*L. vanammei*) against *V. parahaemolyticus* causing AHPND [62–65]. Since it has been reported that there is an interaction between TLR and nanoparticles in mammals [15,65], the expression of TLR3 and ProPO genes was analyzed in the present study. TLR3 and ProPO gene expression in hemocytes from shrimp fed with AuNP was early up-regulated at 24 and 48 h when compared to the control. On this regard, the activation of TLR4 has been reported in human monocytes treated with naked cobalt nanoparticles [67]. Remarkably, it has been hypothesized that different TLRs (TLR3, -4, and -7) are activated by titanium dioxide NP (TiO_2NPs) in mouse, especially TLR4 that is involved in NPs uptake [66]. Regarding effector responses, ProPO gene expression was up-regulated in different tissues of shrimp supplemented with 5–25 nm silver nanoparticles (AgNP) [21]. Although no additional reports about the effect of metallic NP on ProPO gene expression in shrimp are available, it has been reported that organic (chitosan) nanoparticles modulate ProPO gene expression in shrimp fed with NP loaded with the r-VP28 protein [68]. In addition, crayfish (*Procambus clarkii*) fed with chitosan NP for 9 days were protected against WSSV infection, an effect associated to higher proPO oxidase activity in hemolymph [69]. In general, in our study, AuNP modulated immunological responses; demonstrating an early activation (24–48 h) and wide variations in immune responses over time. Interestingly, coincident results have been reported in both *in vitro* and *in vivo* studies using AuNP [17,19]. Moreover, several immunostimulants and probiotics that enhance TLR gene expression and proPO system (activity or gene expression) in shrimp (*L. vanammei*) increased resistance to AHPND and *V. parahaemolyticus* infection [70–72].

Shrimp fed with AuNP at a 2 µg/g dose were protected against a *V. parahaemolyticus* challenge. Curiously, shrimp fed with biosynthesized AgNP of 11.3 ± 2.1 nm were protected against a *Vibrio* sp. infection [73]. Interestingly, survival rates of 71–90% were found in shrimp fed with AgNP after a *V. parahaemolyticus* challenge [21]. In other studies, organic NP also increased the survival rate in several crustaceans after infection with *Vibrio* spp. and viral pathogens [69,74]. In line with these findings, the observed variations on shrimp survival may be due to physicochemical changes in the surface of AuNP that could modify the interactions with the target molecules in shrimp; leading to changes in their uptake, accumulation, and elimination [75,76].

During *V. parahaemolyticus* infection severe atrophy of hepatopancreas with massive detachment of epithelial cells and hemocytic infiltration is observed [5]. Shrimp fed with AuNP and challenged with *V. parahaemolyticus* showed less histopathological damage and hemocytic infiltration when compared to the positive control, mainly in the group immunized with the 2 μg/g dose. To the best of our knowledge, no studies are available describing the effect of NP on hepatopancreas of shrimp challenged with pathogens using quantitative histopathological analysis. However, a decrease in histopathological damage has been reported in shrimps fed with microencapsulated organic acids challenged with *V. harveyi* and *V. parahaemolyticus* [77,78].

In conclusion, the oral administration of naked AuNP (~18 nm) in shrimp showed neither toxicity signs nor histological damage when administered in doses ranging from 0.2 to 20 μg/g; inducing early immunological responses associated to the toll-mediated route through receptor (TLR3) and effector (proPO) gene expression in hemocytes. The 2 μg/g AuNP dose decreased histopathological damages and increased survival in shrimp challenged with *V. parahaemolyticus*, an strain able to cause AHPND. This is the first study on the use of AuNP in shrimp and their effects on immune parameters and protection against an experimental infection with *V. parahaemolyticus*; having relevant implications on the development of attractive approaches to prevent economic losses in aquaculture.

Acknowledgements

The project was funded by CONACYT, Mexico (INFR-2014-01/225924; PDCPN2014-01/248033; FC-2016/2820). Omar González-Ortega edited the English version of the manuscript.

Appendix A. Supplementary data

Supplementary data to this article can be found online at https://doi.org/10.1016/j.fsi.2018.10.056.

References

[1] D.V. Lightner, Disease of cultured penaeid shrimp, Mcvey JP. Handbook of Mariculture, second ed., Crustacean Aquaculture CRC Press, Boca Raton, 1996.
[2] FAO, Report of the FAO/MARD Technical Workshop on Early Mortality Syndrome (EMS) or Acute Hepatopancreatic Necrosis Syndrome (AHPNS) of Cultured Shrimp (under TCP/VIE/3304). Hanoi, Viet Nam, on 25–27 June 2013, 2013 FAO Fisheries and Aquaculture Report No. 1053. Rome. 54 pp http://www.fao.org/docrep/018/i3422e/i3422e.pdf.
[3] S.A. Soto-Rodriguez, B. Gomez-Gil, R. Lozano-Olvera, M. Betancourt-Lozano, M.S. Morales-Covarrubias, Field and experimental evidence of *Vibrio parahaemolyticus* as the causative agent of acute hepatopancreatic necrosis disease (AHPND) of cultured shrimp (*Litopenaeus vannamei*) in northwestern Mexico, Appl. Environ. Microbiol. 81 (2014) 1689–1699.
[4] Y. Li, X. Hu, X. Zhang, Z. Liu, X. Ding, L. Xia, et al., *Photorhabdus luminescens* PirAB-fusion protein exhibits both cytotoxicity and insecticidal activity, FEMS Microbiol. Lett. 356 (2014) 23–31.
[5] H.C. Lai, T.H. Ng, M. Ando, C.T. Lee, I.T. Chen, J.C. Chuang, et al., Pathogenesis of acute hepatopancreatic necrosis disease (AHPND) in shrimp, Fish Shellfish Immunol. 47 (2015) 1006–1014.
[6] T. Defoirdt, P. Sorgeloos, P. Bossier, Alternatives to antibiotics for the control of bacterial disease in aquaculture, Curr. Opin. Microbiol. 14 (2011) 251–258.
[7] M.J.S. Apines-Amar, E.C. Amar, Use of immunostimulants in shrimp culture: an update, in: C.M.A. Caipang, M.B.I. Bacano-Maningas, F.F. Fagutao (Eds.), Biotechnological Advances in Shrimp Health Management in the Philippines, 2015, pp. 45–71 Kerala, India. pp. 45–71.
[8] A.I. Campa-Córdova, N.Y. Hernández-Saavedra, R. De Philippis, F. Ascencio, Generation of superoxide anion and SOD activity in haemocytes and muscle of American white shrimp (*Litopenaeus vannamei*) as a response to β-glucan and sulphated polysaccharide, Fish Shellfish Immunol. 12 (2002) 353–366.
[9] A. Tassanakajon, K. Somboonwiwat, P. Supungul, S. Tang, Discovery of immune molecules and their crucial functions in shrimp immunity, Fish Shellfish Immunol. 34 (2013) 954–967.
[10] K. Söderhäll, L. Cerenius, Crustacean immunity, Annu. Rev. Fish Dis. 2 (1992) 3–23.
[11] M. Shaalan, M. Saleh, M. El-Mahdy, M. El-Matbouli, Recent progress in applications of nanoparticles in fish medicine: a review, Nanomedicine: Nanomedicine: NBM 12 (2016) 701–710.
[12] P. Swain, S.K. Nayak, A. Sasmal, T. Behera, S.K. Barik, S.K. Swain, et al., Antimicrobial activity of metal based nanoparticles against microbes associated with diseases in aquaculture, World J. Microbiol. Biotechnol. 30 (2014) 2491–2502.
[13] T. Kawai, S. Akira, The role of pattern-recognition receptors in innate immunity: update on Toll-like receptors, Nat. Immunol. 11 (2010) 373–384.
[14] F. Li, J. Xiang, Signaling pathways regulating innate immune responses in shrimp, Fish Shellfish Immunol. 34 (2013) 973–980.
[15] Y.H. Luo, L.W. Chang, P. Lin, Metal-based nanoparticles and the immune system: activation, inflammation, and potential applications, BioMed Res. Int. 2015 (2015).
[16] E.Y. Kim, R. Schulz, P. Swantek, K. Kunstman, M.H. Malim, S.M. Wolinsky, Gold nanoparticle-mediated gene delivery induces widespread changes in the expression of innate immunity genes, Gene Ther. 19 (2012) 347–353.
[17] H.J. Yen, S.H. Hsu, C.L. Tsai, Cytotoxicity and immunological response of gold and silver nanoparticles of different sizes, Small 5 (2009) 1553–1561.
[18] S. Lu, D. Xia, G. Huang, H. Jing, Y. Wang, H. Gu, Concentration effect of gold nanoparticles on proliferation of keratinocytes, Colloids Surf., B 81 (2010) 406–411.
[19] J. Małaczewska, The splenocyte proliferative response and cytokine secretion in mice after oral administration of commercial gold nanocolloid, Pol. J. Vet. Sci. 18 (2015) 181–189.
[20] J. Małaczewska, Effect of oral administration of commercial gold nanocolloid on peripheral blood leukocytes in mice, Pol. J. Vet. Sci. 18 (2015) 273–282.
[21] E. Sivaramasamy, W. Zhiwei, F. Li, J. Xiang, Enhancement of vibriosis resistance in *Litopenaeus vannamei* by supplementation of biomastered silver nanoparticles by *Bacillus subtilis*, J. Nanomed. Nanotechnol. 7 (2016) 2.
[22] J. Turkevich, P.C. Stevenson, J. Hillier, A study of the nucleation and growth processes in the synthesis of colloidal gold, Discuss. Faraday Soc. 11 (1951) 55–75.
[23] P. López-León, A. Luna-González, R. Escamilla-Montes, M.D.C. Flores-Miranda, J.A. Fierro-Coronado, P. Álvarez-Ruiz, G. Diarte-Plata, Isolation and characterization of infectious Vibrio parahaemolyticus, the causative agent of AHPND, from the whiteleg shrimp (Litopenaeus vannamei), Lat. Am. J. Aquat. Res. 44 (3) (2016) 470–479.
[24] S. Dangtip, R. Sirikharin, P. Sanguanrut, S. Thitamadee, K. Sritunyalucksana, S. Taengchaiyaphum, et al., AP4 method for two-tube nested PCR detection of AHPND isolates of *Vibrio parahaemolyticus*, Aquacult. Rep. 2 (2015) 158–162.
[25] M. García-Bernal, R. Medina-Marrero, C. Rodríguez-Jaramillo, O. Marrero-Chang, Á.I. Campa-Córdova, R. Medina-García, et al., Probiotic effect of *Streptomyces spp.* on shrimp (*Litopenaeus vannamei*) postlarvae challenged with *Vibrio parahaemolyticus*, Aquacult. Nutr. 24 (2018) 865–871.
[26] M. Reyes-Becerril, C. Guluarte, D. Ceballos-Francisco, C. Angulo, M.Á. Esteban, Enhancing gilthead seabream immune status and protection against bacterial challenge by means of antigens derived from *Vibrio parahaemolyticus*, Fish Shellfish Immunol. 60 (2017) 205–218.
[27] S. Weimer, J. Priebs, D. Kuhlow, M. Groth, S. Priebe, J. Mansfeld, et al., D-Glucosamine supplementation extends life span of nematodes and of ageing mice, Nat. Commun. 5 (2014) 3563.
[28] K.J. Livak, T.D. Schmittgen, Analysis of relative gene expression data using real-time quantitative PCR and the $2^{-\Delta\Delta CT}$ method, Methods 25 (2001) 402–408.
[29] T.A. Bell, D.V. Lightner, A Handbook of Normal Penaeid Shrimp Histology, World Aquaculture Society, 1988, p. 114p.
[30] C.S. Kim, X. Li, Y. Jiang, B. Yan, G.Y. Tonga, M. Ray, et al., Cellular imaging of endosome entrapped small gold nanoparticles, MethodsX 2 (2015) 306–315.
[31] A.I. Campa-Córdova, A.F. León-Gallo, A. Romero-Maldonado, A.C. Ibarra-Serrano, S. Rosales-Mendoza, I. Hirono, et al., Recombinant PirA-like toxin protects shrimp against challenge with *Vibrio parahaemolyticus*, the aetiological agent of acute hepatopancreatic necrosis disease, J. Fish. Dis. 40 (2017) 1725–1729.
[32] S. Eustis, M.A. El-Sayed, Why gold nanoparticles are more precious than pretty gold: noble metal surface plasmon resonance and its enhancement of the radiative and nonradiative properties of nanocrystals of different shapes, Chem. Soc. Rev. 35 (2006) 209–217.
[33] K.S. Lee, M.A. El-Sayed, Gold and silver nanoparticles in sensing and imaging: sensitivity of plasmon response to size, shape, and metal composition, J. Phys. Chem. B 110 (2006) 19220–19225.
[34] D.A. Giljohann, D.S. Seferos, W.L. Daniel, M.D. Massich, P.C. Patel, C.A. Mirkin, Gold nanoparticles for biology and medicine, Angew. Chem. Int. 49 (2010) 3280–3294.
[35] K.J. Hu, P.C. Leung, Food digestion by cathepsin L and digestion-related rapid cell differentiation in shrimp hepatopancreas, Comp. Biochem. Physiol. B Biochem. Mol. Biol. 146 (2007) 69–80.
[36] R. Gibson, P.L. Barker, The decapod hepatopancreas, Oceanogr. Mar. Biol. Annu. Rev. 17 (1979) 285–346.
[37] M. Semmler-Behnke, W.G. Kreyling, J. Lipka, S. Fertsch, A. Wenk, S. Takenaka, et al., Biodistribution of 1.4-and 18-nm gold particles in rats, Small 4 (2008) 2108–2111.
[38] G. Schmid, W.G. Kreyling, U. Simon, Toxic effects and biodistribution of ultrasmall gold nanoparticles, Arch. Toxicol. 91 (2017) 3011–3037.
[39] M.K. Kesarla, B.K. Mandal, P.R. Bandapalli, Gold nanoparticles by *Terminalia bellirica* aqueous extract–a rapid green method, J. Exp. Nanosci. 9 (2014) 825–830.
[40] C. Balalakshmi, K. Gopinath, M. Govindarajan, R. Lokesh, A. Arumugam, N.S. Alharbi, et al., Green synthesis of gold nanoparticles using a cheap Sphaeranthus indicus extract: impact on plant cells and the aquatic crustacean Artemia nauplii, J. Photochem. Photobiol. B Biol. 173 (2017) 598–605.
[41] L.M. Skjolding, G. Ašmonaitė, R.I. Jølck, T.L. Andresen, H. Selck, A. Baun, J. Sturve, An assessment of the importance of exposure routes to the uptake and internal localisation of fluorescent nanoparticles in zebrafish (*Danio rerio*), using light sheet microscopy, Nanotoxicology 11 (2017) 351–359.
[42] N. Li, Y. Zhao, J. Yang, Impact of waterborne copper on the structure of gills and hepatopancreas and its impact on the content of metallothionein in juvenile giant

freshwater prawn *Macrobrachium rosenbergii* (Crustacea: Decapoda), Arch. Environ. Contam. Toxicol. 52 (2007) 73.
[43] M.G. Frías-Espericueta, S. Abad-Rosales, A.C. Nevárez-Velázquez, I. Osuna-López, F. Páez-Osuna, R. Lozano-Olvera, et al., Histological effects of a combination of heavy metals on Pacific white shrimp *Litopenaeus vannamei* juveniles, Aquat. Toxicol. 89 (2008) 152–157.
[44] M.G. Frías-Espericueta, R. Castro-Longoria, G.J. Barrón-Gallardo, J.I. Osuna-López, S.M. Abad-Rosales, F. Páez-Osuna, et al., Histological changes and survival of Litopenaeus vannamei juveniles with different copper concentrations, Aquaculture 278 (2008) 97–100.
[45] X.D. Zhang, H.Y. Wu, D. Wu, Y.Y. Wang, J.H. Chang, Z. Zhai, et al., Toxicologic effects of gold nanoparticles in vivo by different administration routes, Int. J. Nanomed. 5 (2010) 771–781.
[46] K. Lindfors, T. Kalkbrenner, P. Stoller, V. Sandoghdar, Detection and spectroscopy of gold nanoparticles using supercontinuum white light confocal microscopy, Phys. Rev. Lett. 93 (2004) 037401.
[47] N. Khlebtsov, L. Dykman, Biodistribution and toxicity of engineered gold nanoparticles: a review of in vitro and in vivo studies, Chem. Soc. Rev. 40 (2011) 1647–1671.
[48] N.M. Wade, N. Bourne, C.J. Simon, Influence of marker particle size on nutrient digestibility measurements and particle movement through the digestive system of shrimp, Aquaculture 491 (2018) 273–280.
[49] C. Schleh, M. Semmler-Behnke, J. Lipka, A. Wenk, S. Hirn, M. Scha er, et al., Size and surface charge of gold nanoparticles determine absorption across intestinal barri- ers and accumulation in secondary target organs after oral administration, Nanotoxicology 6 (2012) 36–46.
[50] H.H. Sung, G.H. Kou, L. Song, Vibriosis resistance induced by glucan treatment in tiger shrimp (*Penaeus monodon*), Fish Pathol. 29 (1994) 11–17.
[51] Y.L. Song, Y.T. Hsieh, Immunostimulation of tiger shrimp (*Penaeus monodon*) hemocytes for generation of microbicidal substances: analysis of reactive oxygen species, Dev. Comp. Immunol. 18 (1994) 201–209.
[52] H.H. Sung, Y.L. Yang, L. Song, Enhancement of microbicidal activity in the tiger shrimp *Penaeus monodon* via immunostimulation, J. Crustac Biol. 16 (1996) 278–284.
[53] Y.L. Song, C.C. Huang, Application of immunostimulants to prevent shrimp diseases, Recent Adv. Mar. Biotechnol. 5 (1999) 173–187.
[54] Z.F. Zhang, M. Shao, K.H. Kang, Classification of haematopoietic cells and haemocytes in Chinese prawn *Fenneropenaeus chinensis*, Fish Shellfish Immunol. 21 (2006) 159–169.
[55] P.F. Ji, C.L. Yao, Z.Y. Wang, Reactive oxygen system plays an important role in shrimp *L. vannamei* defense against *V. parahaemolyticus* and WSSV infection, Dis. Aquat. Org. 96 (2011) 9–20.
[56] D. Gonçalves-Soares, J. Zanette, J.S. Yunes, G.M. Yepiz-Plascencia, A.C. Bainy, Expression and activity of glutathione S-transferases and catalase in the shrimp *Litopenaeus vannamei* inoculated with a toxic *Microcystis aeruginosa* strain, Mar. Environ. Res. 75 (2012) 54–61.
[57] T. Muralisankar, P.S. Bhavan, S. Radhakrishnan, C. Seenivasan, V. Srinivasan, The effect of copper nanoparticles supplementation on freshwater prawn *Macrobrachium rosenbergii* post larvae, J. Trace Elem. Med. Biol. 34 (2016) 39–49.
[58] S. Akira, S. Uematsu, O. Takeuchi, Pathogen recognition and innate immunity, Cell 124 (2006) 783–801.
[59] P.H. Wang, J.P. Liang, Z.H. Gu, D.H. Wan, S.P. Weng, X.Q. Yu, et al., Molecular cloning, characterization and expression analysis of two novel Tolls (LvToll2 and LvToll3) and three putative Spätzle-like Toll ligands (LvSpz1–3) from *Litopenaeus vannamei*, Dev. Comp. Immunol. 36 (2012) 359–371.
[60] L. Vazquez, J. Alpuche, G. Maldonado, C. Agundis, A. Pereyra-Morales, E. Zenteno, Immunity mechanisms in crustaceans, Innate Immun. 15 (2009) 179–188.
[61] P. Amparyup, W. Charoensapsri, A. Tassanakajon, Prophenoloxidase system and its role in shrimp immune responses against major pathogens, Fish Shellfish Immunol. 34 (2013) 990-100.
[62] X.P. Hong, D. Xu, Y. Zhuo, H.Q. Liu, L.Q. Lu, Identification and pathogenicity of *Vibrio parahaemolyticus* isolates and immune responses of Penaeus (*Litopenaeus*) *vannamei* (Boone), J. Fish. Dis. 39 (2016) 1085–1097.
[63] W. Soonthornchai, S. Chaiyapechara, S. Klinbunga, W. Thongda, S. Tangphatsornruang, T. Yoocha, et al., Differentially expressed transcripts in stomach of *Penaeus monodon* in response to AHPND infection, Dev. Comp. Immunol. 65 (2016) 53–63.
[64] R.A. Raja, R. Sridhar, C. Balachandran, A. Palanisammi, S. Ramesh, K. Nagarajan, Pathogenicity profile of *Vibrio parahaemolyticus* in farmed Pacific white shrimp, *Penaeus vannamei*, Fish Shellfish Immunol. 67 (2017) 368–381.
[65] Z. Zheng, F. Wang, J.J. Aweya, R. Li, D. Yao, M. Zhong, et al., Comparative transcriptomic analysis of shrimp hemocytes in response to acute hepatopancreas necrosis disease (AHPND) causing *Vibrio parahemolyticus* infection, Fish Shellfish Immunol. 74 (2018) 10–18.
[66] P. Chen, K. Kanehira, A. Taniguchi, Role of toll-like receptors 3, 4 and 7 in cellular uptake and response to titanium dioxide nanoparticles, Sci. Technol. Adv. Mater. 14 (2013) 015008.
[67] P.A. Potnis, D.K. Dutta, S.C. Wood, Toll-like receptor 4 signaling pathway mediates proinflammatory immune response to cobalt-alloy particles, Cell. Immunol. 282 (2013) 53–65.
[68] G. Taju, D.V. Kumar, S.A. Majeed, S. Vimal, S. Tamizhvanan, S.S. Kumar, et al., Delivery of viral recombinant VP28 protein using chitosan tripolyphosphate nanoparticles to protect the whiteleg shrimp, *Litopenaeus vannamei* from white spot syndrome virus infection, Int. J. Biol. Macromol. 107 (2018) 1131–1141.
[69] B. Sun, H. Quan, F. Zhu, Dietary chitosan nanoparticles protect crayfish *Procambarus clarkii* against white spot syndrome virus (WSSV) infection, Fish Shellfish Immunol. 54 (2016) 241–246.
[70] M. Sivagnanavelmurugan, B.J. Thaddaeus, A. Palavesam, G. Immanuel, Dietary effect of *Sargassum wightii* fucoidan to enhance growth, prophenoloxidase gene expression of *Penaeus monodon* and immune resistance to *Vibrio parahaemolyticus*, Fish Shellfish Immunol. 39 (2014) 439–449.
[71] D.M. Félix, J.A. Elías, Á.I. Córdova, L.R. Córdova, A. González, E.C. Jacinto, et al., Survival of *Litopenaeus vannamei* shrimp fed on diets supplemented with *Dunaliella sp*. is improved after challenges by *Vibrio parahaemolyticus*, J. Invertebr. Pathol. 148 (2017) 118–123.
[72] S. Chomwong, W. Charoensapsri, P. Amparyup, A. Tassanakajon, Two host gut-derived lactic acid bacteria activate the proPO system and increase resistance to an AHPND-causing strain of *Vibrio parahaemolyticus* in the shrimp *Litopenaeus vannamei*, Dev. Comp. Immunol. 89 (2018) 54–65, https://doi.org/10.1016/j.dci.2018.08.002.
[73] K. Kandasamy, N.M. Alikunhi, G. Manickaswami, A. Nabikhan, G. Ayyavu, Synthesis of silver nanoparticles by coastal plant *Prosopis chilensis* (L.) and their efficacy in controlling vibriosis in shrimp *Penaeus monodon*, Appl. Nanosci. 3 (2013) 65–73.
[74] S. Ufaz, A. Balter, C. Tzror, S. Einbender, O. Koshet, J. Shainsky-Roitman, et al., Anti-viral RNAi nanoparticles protect shrimp against white spot disease, Mol. Syst. Des. Eng. 3 (2018) 38–48.
[75] A.E. Nel, L. Mädler, D. Velegol, T. Xia, E.M. Hoek, P. Somasundaran, et al., Understanding biophysicochemical interactions at the nano–bio interface, Nat. Mater. 8 (2009) 543–557.
[76] M.A. Dobrovolskaia, A.K. Patri, J. Zheng, J.D. Clogston, N. Ayub, P. Aggarwal, et al., Interaction of colloidal gold nanoparticles with human blood: effects on particle size and analysis of plasma protein binding profiles, Nanomed. Nanotechnol. 5 (2009) 106–117.
[77] N. Romano, C.B. Koh, W.K. Ng, Dietary microencapsulated organic acids blend enhances growth, phosphorus utilization, immune response, hepatopancreatic integrity and resistance against *Vibrio harveyi* in white shrimp, *Litopenaeus vannamei*, Aquaculture 435 (2015) 228–236.
[78] T. Rudtanatip, N. Boonsri, S. Asuvapongpatana, B. Withyachumnarnkul, K. Wongprasert, A sulfated galactans supplemented diet enhances the expression of immune genes and protects against *Vibrio parahaemolyticus* infection in shrimp, Fish Shellfish Immunol. 65 (2017) 186–197.